SUPPLEMENTARY INFORMATION

Probing conformational states of the finger and thumb subdomains of HIV-1 reverse transcriptase using double electron-electron resonance EPR spectroscopy

Thomas Schmidt,[1] Lan Tian,[2] and G. Marius Clore[1,*]

Laboratories of [1]Chemical Physics and [2]Molecular Biology, National Institute of Diabetes and Digestive and Kidney Diseases, National Institutes of Health, Bethesda, MD 20892-0520.

Experimental, 5 Tables and 13 Figures.

EXPERIMENTAL

p66 and p51 expression, protein purification, nitroxide spin-labeling and EPR sample preparation. Plasmids encoding His-tagged the p66 or p51 subunits of HIV-1 RT with a HRV 3C protease cleavage site between the tag and the N-terminus of p66 or p51 were a gift from Dr. Wei Yang. Site-directed mutagenesis to introduce surface-exposed cysteine residues and/or replace the native cysteines of p66 by Ala was carried out using the QuickChange Site-directed Mutagenesis kit (Stratagene). Four constructs, each containing two surface-exposed cysteines for spin-labeling, one in the finger subdomain, the other in the thumb subdomain, were generated: wild-type with C38/C280; C38/A304C with C280A; W24C/C280 with C38A; and T39C/E308C with C38A and C280A. Expression, uniform deuterium labeling (99%), purification and nitroxide spin-labeling with MTSL (Toronto Research Chemicals) was carried out exactly as described previously.[1] The concentrations of spin-labeled p66 and unlabeled p51 (both fully deuterated, 99 atom %D) used in the DEER experiments was 50 and 350 μM, respectively, in 25 mM Tris-HCl, pH 8,100 mM NaCl, 20 mM MgCl, 30% (w/v) deuterated (1,1,2,3,3-d5, 99 atom % D) glycerol, 70% (v/v) D_2O (99.9 atom % D). DNA oligonucleotides were purchased from Invitrogen. Complexes of p66/p51 with a 24-base pair DNA duplex containing a 3' overhang (5'-CGTATGCCTATAGTTATTGTGGCC-3'; 5'-ATGATGGCCACAATAACTATAGGCATA-3') was obtained by addition of lyophilized DNA to a final concentration of 500 μM. Complexes with NNTRIs (purchased from Toronto Research Chemicals Inc.) were prepared by addition of the appropriate aliquot from 50 mM stock NNRTI solutions in deuterated DMSO (99.9 atom %D), for a final NNRTI concentration of 1 mM. Samples (15 μl) for EPR were pipetted into 1 mm diameter quartz EPR tubes (VitroCom Inc.) and flash frozen in liquid nitrogen.

HIV-1 RT DNA/RNA binding assay. A fluorescence polarization assay was used to measure the affinity of the various HIV-1 RT nitroxide spin-labeled constructs.[2] The RNA/DNA hybrid duplex was 22 base pairs long, with five and four nucleotide overhangs at the 5'- and 3'-ends of the RNA strand, respectively. The RNA strand was labeled at the 3'-end with 6-carboxyfluorescein (6-FAM). 10 nM RNA/DNA was mixed with HIV-RT in the mixing buffer containing 0.1 mg/mL bovine serum albumin, 50 mM Tris-HCl, pH 8, 1 mM dithiotreitol (DTT), 0.1 mM ethylenediamine tetraacetic (EDTA) acid and 1 mM $CaCl_2$ for 10 min at 16°C, prior to measuring fluorescence polarization on a CLARIOstar (BMG Labtech) fluorescence plate reader ($\lambda_{excitation}$ = 482 nm, pathlength = 16 nm; and $\lambda_{emission}$ = 530 nm, pathlength = 40 nm). The data were fit to a one-binding site model by non-linear least-squares.

Polymerase assay. The RNA/DNA hybrid was a 22-base pair duplex with a three nucleotide overhang at the 5'-end of the RNA strand. The DNA strand was labeled at the 5'-end with 6-FAM. The polymerase activity of the various HIV-1 spin-labeled p66/p51 constructs was assayed by monitoring elongation of the RNA/DNA hybrid by one nucleotide.[3] 66 nM HIV-1 RT was mixed with 33 nM DNA/RNA hybrid, and incubated at 16°C in mixing buffer (0.1 mg/mL BSA, 50 mM Tris-HCl, pH 8, 50 mM KCl and 1 mM DTT). The reaction was initiated by addition of 1.3 mM $MgCl_2$ and 0.1 mM ATP. The reaction was stopped after 10 sec by addition of an equal volume of 90% (v/v) formamide, 0.025% sodium dodecylsulfate and 50 mM EDTA, denatured at 95 °C for 3 min, and resolved by TBE-Urea gel electrophoresis. The resulting bands were visualized using the Typhoon FLA 9500 biomolecular imager in fluorescence mode ($\lambda_{excitation}$=490 nm, $\lambda_{emission}$=520 nm, LBP filter).

Pulsed DEER EPR spectroscopy. Pulsed EPR data were collected at Q-band (33.8 GHz) at 50 K on a Bruker E-580 spectrometer equipped with a 150 W traveling-wave tube amplifier, a model ER5107D2 resonator, and a cryofree cooling unit. Samples were placed in 1 mm internal diameter quartz tubes (VitroCom) and flash frozen in liquid nitrogen. DEER experiments were acquired with a conventional four-pulse sequence.[4] The observer and ELDOR pump pulses were separated by ca. 90 MHz with the observe π/2 and π pulses set to 12 and 24 ns, respectively, and

the ELDOR π pulse to 8 ns. The pump frequency was centered at the Q-band nitroxide spectrum located at +40 MHz from the center of the resonator frequency. The τ_1 value of 400 ns for the first echo-period time was incremented eight times in 16 ns steps to average ^{2}H modulation; the position of the ELDOR pump pulse was incremented in steps of Δt =14 ns. The bandwidth of the overcoupled resonator was 120 MHz. The second echo period time τ_2 was set to t_{max} + 700 ns, where t_{max} is the maximum dipolar acquisition time; data collection was not extended to the full τ_2 range because of a persistent "2+1" echo perturbation of the DEER echo curves at a time of about τ_1 from the final observe π pulse.[5] The length of t_{max} employed ranged from 6 to 20 μs, depending on signal-to-noise of the sample. The pulse gate time used for echo integration was 32–38 ns. Typical total acquision times ranged from 12-16 hrs.

Predicted P(r) distance distributions between spin labeled from crystal structures. The program SCWRL4.0 was used to optimize side chain positions before loading the crystal structure coordinates into the MMMv2013.2 program[6] to generate rotamer probabilities for each spin-label pair from which raw $P(r)$ distributions were obtained from a histogram of the resulting distances between spin labels. The raw distributions were then converted to a Gaussian representation.

P(r) distributions from DEER data. The Q-band DEER four-pulse echo curves were primarily analyzed using the program DD[7] to derive $P(r)$ distributions using a sum of Gaussians to directly fit the experimental DEER data (including automated background correction with a best-fit exponential decay). The optimal number of Gaussians required to represent the DEER data was assessed using the Akaike information criterion corrected for finite sample size (AICc) and the Bayesian information criterion (BIC).[8] In a number of instances a broad underlying component represented by a second or third Gaussian was required to fit the DEER echo curves; such broad underlying components can be attributed to some degree of aggregation resulting in a wide distribution of distances, and hence a large width of the DEER-derived $P(r)$ distribution, due to random spin label placement within a spatially defined aggregate.[9] The mean distance values arising from specific intramolecular interactions between spin labels are not significantly different for two and three Gaussian fits and are characterized by low 2σ values (see Tables S2-S5). Broad distance distributions arising from aggregates are easily identified through either large 2σ values for the mean distance and/or width; in addition for some of the three Gaussian fits, spikes are observed with very narrow widths (~0.2 Å) that are readily discarded even if the AICc and BIC criteria show improvement (Tables S2-S5).

$P(r)$ distributions were also generated by validated Tikhonov regularization using DeerAnalysis 2016,[10] and are shown in Figs. S12 and S13. Validation was carried out using the DeerAnalysis validation tool varying the modulation depth (11 steps), background density (11 steps) and background start (11 steps) for a total of 1331 permutations. The Tikhonov regularization parameter α was automatically determined by DeerAnalysis for each iteration, and the value of α ranged from 10 to 100. The position of a given $P(r)$ maximum and width was determined by evaluating the mean and width delineated by the dashed lines in Figs. S12 and S13. Although the Tikhonov-derived $P(r)$ distributions are much noisier than those obtained from DD,[7] the resulting mean distance values and associated widths are not significantly different from those obtained by Gaussian analysis (Tables S2-S5).

Table S1. PDB codes and citations of HIV RT crystal structures used in the current study.

Conformation of finger/ thumb subdomains of p66 subunit[a]	PDB code	State	Reference
Closed I	1DLO	unliganded	*12*
	1HQE	unliganded	*13*
	2IAJ	unliganded	*14*
	1MU2	unliganded	*15*
	4ZHR	unliganded	*16*
	1QE1	unliganded	*17*
Closed II	3DLK	unliganded	*18*
	3IG1	unliganded	*19*
	4DG1	unliganded	*20*
Partially-open	5TXL	+ DNA + dATP	*21*
	5TXM	+ DNA + ddATP	*21*
	3V4I	+ DNA + AZT triphosphate	*22*
	3KJV	+ DNA terminated by ddCMP	*23*
	3KK3	+ GS9148 terminated DNA primer	*23*
Open I	3QIP	+ nevirapine	*24*
	1IKW	+ efavirenz	*25*
	4G1Q	+ rilpiviridine	*26*
	1KLM	+ delavirdine	*27*
	1SV5	+ etravirine	*28*
	1JLE	unliganded drug resistance Y188C mutant	*29*
Open II	4B3O	+ RNA/DNA + efavirenz	*30*
	3V81	+ DNA + efavirenz	*31*

[a]See Table 1 of main text.

Table S2. Comparison of DEER-derived $P(r)$ distance distributions for the C38-R1/C280-R1 RT construct obtained from one, two and three Gaussian fits using DD[7] and from validated Tikhonov regulation using DeerAnalysis.[10,a]

State	Gaussians	Mean distance (2σ)[b] (Å)	Width (2σ)[b] (Å)	AICc[c]	BIC[c]
Unliganded					
Gaussian fit	1	56 (0.2)	7 (0.2)	-10680	-10651
	2a	56 (0.2)	3 (0.4)	-11018	-10974
	2b	56 (0.9)	13 (2.0)		
	3a	42 (6.4)	7 (5.2)	-10102	-10052
	3b	58 (1.0)	5 (0.6)	-10102	-10052
	3c	63 (6.9)	0.2 (97.3)		
Tikhonov		57	5		
+ *DNA*					
Gaussian fit	1	55 (0.1)	6 (0.1)	-5003	-4977
	2a	52 (0.7)	9 (0.6)	-5154	-5116
	2b	56 (0.1)	4 (0.2)		
	3a	40 (5.9)	8 (4.9)	-5010	-5051
	3b	56 (0.3)	5 (0.3)		
	3c	56 (0.3)	0.2 (4.3)		
Tikhonov		54	8		
+ *Etravirine*					
Gaussian fit	1	46 (0.1)	4 (0.1)	-10660	-10631
	2a	45 (0.2)	6 (0.3)	-10870	-10826
	2b	48 (0.8)	7 (0.5)		
	3a	38 (11.1)	18 (8.9)	-11457	-11398
	3b	45 (0.9)	3 (0.9)		
	3c	49 (3.6)	5 (3.6)		
Tikhonov		46	4		
+ *Rilpivirine*					
Gaussian fit	1	46 (0.1)	4 (0.1)	-10846	-10817
	2a	46 (0.1)	6 (0.1)	-11103	-11059
	2b	49 (3)	14 (2.2)		
	3a	45 (9.6)	19 (9.5)		
	3b	45 (0.4)	3 (0.3)		
	3c	52 (22.9)	5 (11.4)		
Tikhonov		45	3		

Table S2 (cont.)

State	Gaussians	Mean distance (2σ) (Å)	Width (2σ) (Å)	AICc[b]	BIC[b]
+ ***Delavirdine***					
Gaussian fit	1	46 (0.1)	4 (0.1)	-11250	-11221
	2a	46 (0.1)	3 (0.2)	-11655	-11611
	2b	49 (1.0)	7 (0.5)		
	3a	45 (1.2)	3 (0.6)	-12230	-12172
	3b	47 (1.3)	10 (1.9)		
	3c	49 (10)	3 (4.0)		
Tikhonov		46	4		
+ ***Efavirenz***					
Gaussian fit	1	47 (0.2)	4 (0.2)	-9564	-9535
	2a	47 (0.3)	4 (0.4)	-9582	-9539
	2b	50 (33)	9 (19)		
	3a	44 (4.6)	3 (1.9)	-10066	-10008
	3b	45 (9.5)	11 (12)		
	3c	49 (9.3)	3 (3.8)		
Tikhonov		47	4		
+ ***Nevirapine***					
Gaussian fit	1	48 (0.2)	6 (0.3)	-8895	-8866
	2a	48 (0.3)	6 (0.5)	-9002	-8958
	2b	55 (11)	20 (7.0)		
	3a	46 (3.9)	3 (2.2)	-9463	-9404
	3b	52 (3.1)	2 (1.7)		
	3c	54 (8.5)	18 (5.4)		
Tikhonov		48	5		

[a]The mean distances and widths highlighted in yellow correspond to specific intramolecular interactions between spin labels.
[b]2σ = 2 standard deviations. Note that 2σ is a measure of the precision (and not the accuracy) with which the mean distance or width is determined.
[c]AICc, sample size corrected Akaike information criterion; BIC, Bayesian information criterion.

Table S3. Comparison of DEER-derived $P(r)$ distance distributions for the C38-R1/A304C-R1 RT construct obtained from one, two and three Gaussian fits using DD[7] and from validated Tikhonov regulation using DeerAnalysis.[10,a]

State	Gaussians	Mean distance (2σ) (Å)	Width (2σ) (Å)	AICc[b]	BIC[b]
Unliganded					
Gaussian fit	1	84 (0.8)	16 (1.1)	-9747	-9718
	2a	42(1.7)	8 (2.4)	-10048	-10050
	2b	83 (0.3)	9 (0.7)		
	3a	42 (2.8)	10.5 (4.1)	-10630	-10571
	3b	79 (1.3)	0.3 (18)		
	3c	88 (5.6)	12.3 (5.6)		
Tikhonov		45	6		
		84	7		
+ *DNA*					
Gaussian fit	1	89 (1.9)	21 (1.6)	-10232	-10202
	2a	82 (119)	50 (74)	-10501	-10457
	2b	84 (0.4)	8 (0.7)		
	3a	43 (2.0)	6.8 (3.2)	-10503	-10444
	3b	83 (5)	10 (4.9)		
	3c	100 (430)	0.2 (208)		
Tikhonov		85	7		
+ *Etravirin*e					
Gaussian fit	1	58 (0.2)	10 (0.3)	-8466	-8437
	2a	56 (0.5)	6 (0.8)	-8857	-8814
	2b	79 (19)	24 (10)		
	3a	57 (1.1)	0.3 (9.7)	-9318	-9259
	3b	56 (0.8)	8 (1.3)		
	3c	85 (43)	6 (51)		
Tikhonov		55	8		
		76	4		
+ *Rilpivirine*					
Gaussian fit	1	58 (0.2)	11 (0.2)	-8809	-8780
	2a	56 (0.3)	5 (0.4)	-9561	-9517
	2b	73 (5.3)	23 (3.8)		
	3a	56 (1.0)	5 (0.8)	-10049	-9990
	3b	70 (180)	22 (750)		
	3c	100 (390)	27 (120)		
Tikhonov		56	6		
		76	4		

Table S3 (cont.)

State	Gaussians	Mean distance (2σ) (Å)	Width (2σ) (Å)	AICc[b]	BIC[b]
+ *Delavirdine*					
Gaussian fit	1	59 (0.2)	11 (0.2)	-8417	-8388
	2a	56 (0.5)	6 (0.3)	-9005	-8962
	2b	76 (1.9)	4 (7.5)		
	3a	24 (5.8)	15 (12.3)	-8203	-8144
	3b	54 (3.6)	0.2 (32)		
	3c	61 (1.4)	10 (0.8)		
Tikhonov		55	6		
		76	3		
+ *Efavirenz*					
Gaussian fit	1	58 (0.2)	10 (0.3)	-8374	-8345
	2a	56 (0.5)	6 (0.8)	-8772	-8729
	2b	82 (12)	18 (11)		
	3a	55 (0.8)	4.3 (1.5)	-9134	-9075
	3b	62 (17)	14 (11)		
	3c	77 (74)	0.4 (610)		
Tikhonov		56	6		
		76	4		
+ *Nevirapine*					
Gaussian fit	1	58 (0.2)	13 (0.3)	-8912	-8883
	2a	55 (0.2)	4 (0.3)	-9846	-9802
	2b	78 (4)	25 (3.1)		
	3a	55 (0.6)	4 (0.5)	-10062	-10003
	3b	76 (120)	40 (77)		
	3c	84 (5.6)	3 (7.1)		
Tikhonov		55	6		
		76	3		

[a]The mean distances and widths highlighted in yellow correspond to specific intramolecular interactions between spin labels.
[b]AICc, sample size corrected Akaike information criterion; BIC, Bayesian information criterion.

Table S4. Comparison of DEER-derived $P(r)$ distance distributions for the W24C-R1/C280-R1 RT construct obtained from one, two and three Gaussian fits using DD[7] and from validated Tikhonov regulation using DeerAnalysis 2016.[10,a]

State	Gaussians	Mean distance (2σ) (Å)	Width (2σ) (Å)	AICc[b]	BIC[b]
Unliganded					
Gaussian fit	1	15 (2.2)	22 (1)	-11296	-11267
	2a	22 (0.3)	5 (0.5)	-11905	-11861
	2b	42 (2.1)	14 (1.3)		
	3a	22 (0.3)	4 (0.9)	-12628	-12570
	3b	36 (5.9)	11 (6.7)		
	3c	59 (1.5)	4 (1.5)		
Tikhonov		21	6		
+ *DNA*					
Gaussian fit	1	45 (0.5)	12 (0.5)	-10186	-10052
	2a	38 (1.6)	25 (1.6)	-10340	-10298
	2b	46 (0.2)	5 (0.4)		
	3a	29 (32)	17 (29)	-10092	-10034
	3b	45 (230)	37 (90)		
	3c	47 (0.4)	5 (0.5)		
Tikhonov		45	7		
+ *Etravirine*					
Gaussian fit	1	43 (0.3)	15 (0.2)	-11256	-11227
	2a	40 (1.5)	24 (1.6)	-12444	-12400
	2b	46 (0.2)	4 (0.4)		
	3a	29 (33)	17 (30)	-13092	-13034
	3b	45 (250)	37 (97)		
	3c	47 (0.4)	5 (0.5)		
Tikhonov		44	5		
+ *Rilpivirine*					
Gaussian fit	1	44 (0.4)	15 (0.4)	-11078	-11049
	2a	15 (28)	49 (17)	-11752	-11708
	2b	46 (0.4)	4 (0.6)		
	3a	37 (23)	16 (23)	-12378	-12319
	3b	47 (1.2)	6 (1.6)		
	3c	80 (350)	52 (615)		
Tikhonov		45	7		

State	Gaussians	Mean distance (2σ) (Å)	Width (2σ) (Å)	AICc[b]	BIC[b]
+ *Delavirdine*					
Gaussian fit	1	41 (0.4)	15 (0.4)	-10961	-10932
	2a	43 (0.3)	4 (0.4)	-11490	-11446
	2b	53 (23)	48 (33)		
	3a	36 (12)	15 (12)	-12291	-12232
	3b	45 (0.8)	5 (1.1)		
	3c	78 (216)	51 (414)		
Tikhonov		45	8		
+ *Efavirenz*					
Gaussian fit	1	44 (0.6)	12 (0.6)	-9884	-9854
	2a	44 (12)	24 (30)	-9896	-9852
	2b	45 (1.2)	6 (3.4)		
	3a	39 (1600)	19 (2100)	-9880	-9882
	3b	44 (11)	9 (26)		
	3c	52 (920)	23 (1100)		
Tikhonov		44	9		
+ *Nevirapine*					
Gaussian fit	1	45 (0.2)	8 (0.3)	-10371	-10341
	2a	43 (22)	43 (25)	-10871	-10827
	2b	45 (0.3)	4 (0.4)		
	3a	20 (28)	12 (57)	-10046	-9987
	3b	46 (1.8)	6 (3.3)		
	3c	50 (50)	25 (26)		
Tikhonov		45	7		

[a]The mean distances and widths highlighted in yellow correspond to specific intramolecular interactions between spin labels.
[b]AICc, sample size corrected Akaike information criterion; BIC, Bayesian information criterion.

Table S5. Comparison of DEER-derived $P(r)$ distance distributions for the T39C-R1/E308C-R1 RT construct obtained from one, two and three Gaussian fits using DD[7] and from validated Tikhonov regulation using DeerAnalysis[10,a]

State	Gaussians	Mean distance (2σ) (Å)	Width (2σ) (Å)	AICc[b]	BIC[b]
Unliganded					
Gaussian fit	1	54 (0.1)	7 (0.1)	-9893	-9864
	2a	53 (0.1)	3 (0.1)	-11436	-11393
	2b	58 (0.9)	20 (1.6)		
	3a	53 (0.5)	4 (0.2)		
	3b	61 (38)	24 (16)		
	3c	85 (33)	0.3 (527)		
Tikhonov		53	5		
+ *DNA*					
Gaussian fit	1	67 (01)	7 (0.2)	-6911	-6884
	2a	65 (0.5)	11 (0.7)	-7258	-7217
	2b	68 (0.2)	3 (0.6)		
	3a	60 (8.7)	10 (4)	-7378	-7320
	3b	68 (0.2)	3 (0.6)		
	3c	95 (49)	12 (71)		
+ *Etravirine*					
Gaussian fit	1	67 (0.1)	7 (0.1)	-9394	-9365
	2a	65 (0.7)	17 (1.6)	-10003	-9960
	2b	67 (0.1)	3 (0.2)		
	3a	60 (8.7)	10 (4)	-7378	-7320
	3b	68 (0.2)	3 (0.6)		
	3c	95 (49)	12 (71)		
Tichonov		64	8		
+ *Rilviripine*					
Gaussian fit	1	67 (0.1)	7 (0.2)	-9367	-9338
	2a	65 (0.5)	12 (0.7)	-9808	-9764)
	2b	67 (0.1)	3 (0.2)		
	3a	62 (9.8)	9 (6.4)	-9868	-9810
	3b	69 (0.3)	3 (0.9)		
	3c	106 (273)	22 (224)		
Tikhonov		65	7		

Table S5 (cont.)

State	Gaussians	Mean distance (2σ) (Å)	Width (2σ) (Å)	AICc[b]	BIC[b]
+ Delavirdine					
Gaussian fit	1	66 (0.1)	5 (0.1)	-9617	-9588
	2a	62 (1.8)	23 (3.4)	-10739	-10696
	2b	66 (0.1)	3 (0.1)		
	3a	55 (3.6)	8 (2.7)	-11078	-11020
	3b	67 (0.1)	3 (0.2)		
	3c	99 (40)	12 (22)		
Tickonov		63	7		
+ Efavirenz					
Gaussian fit	1	65 (0.1)	9 (0.2)	-9018	-9019
	2a	66 (3.5)	35 (4.5)	-9784	-9755
	2b	67 (0.1)	4 (0.1)		
	3a	52 (4.9)	8 (3.6)		
	3b	66 (0.3)	4 (0.3)		
	3c	101 (56)	8 (21)		
Tikhonov		63	7		
+ Nevirpine					
Gaussian fit	1	65 (0.1)	7 (0.1)	-9501	-9472
	2a	66 (0.1)	3 (0.3)	-10128	-10084
	2b	67 (0.8)	19 (2.3)		
	3a	51 (1.0)	4 (1.1)	-10402	-10344
	3b	65 (0.2)	4 (0.2)		
	3c	101 (61)	12 (30)		
Tikhonov		65	8		

[a]The mean distances and widths highlighted in yellow correspond to specific intramolecular interactions between spin labels.
[b]AICc, sample size corrected Akaike information criterion; BIC, Bayesian information criterion.

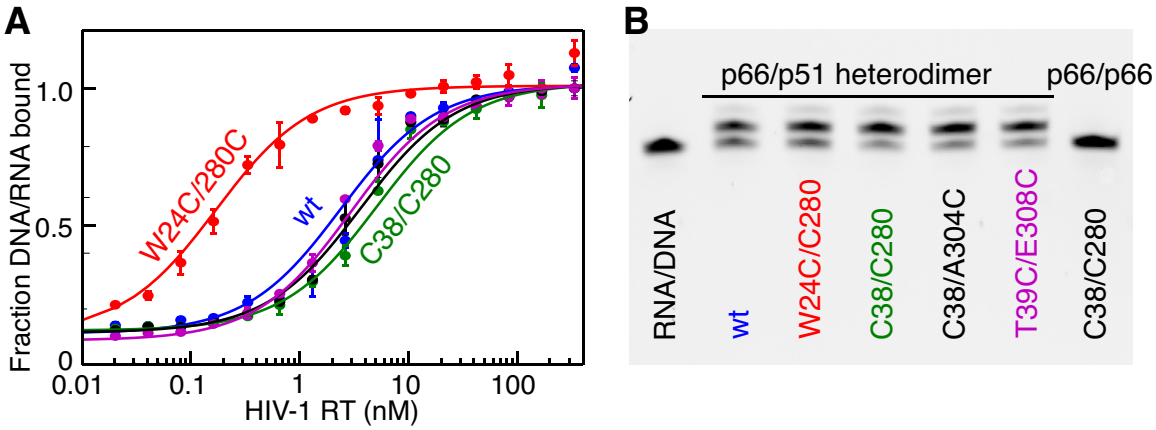

Figure S1. DNA/RNA binding and polymerase activity of HIV-1 RT wild type and nitroxide spin-labeled (R1) constructs. (A) Binding of 5'-fluorescein labeled DNA/RNA to wild type and doubly spin-labeled HIV-1 RT (note only the p66 subunit is doubly spin-labeled). The color coding is as follows: blue, wild type; green, C38-R1/C280-R1 construct; black, C38-R1/A304C-R1 construct; red; W24C-R1/C280-R1 construct; and purple, T39C-R1/E308C-R1 construct. For simplicity R1 has been omitted in the figure. (B) Gel (20% TBE-Urea) electrophoresis polymerase assay monitoring elongation of an RNA/DNA hybrid by one nucleotide. All p66/p51 heterodimers containing a doubly spin-labeled p66 subunit are active, while the p66/p66 homodimer (right-most lane), as expected, has no polymerase activity. (See SI Experimental for details). Color coding as in panel A. It is also worth noting that previous work has shown that the two cysteines at positions 38 and 280 are dispensable and do not significantly impact nucleic acid binding or polymerase activity.[11]

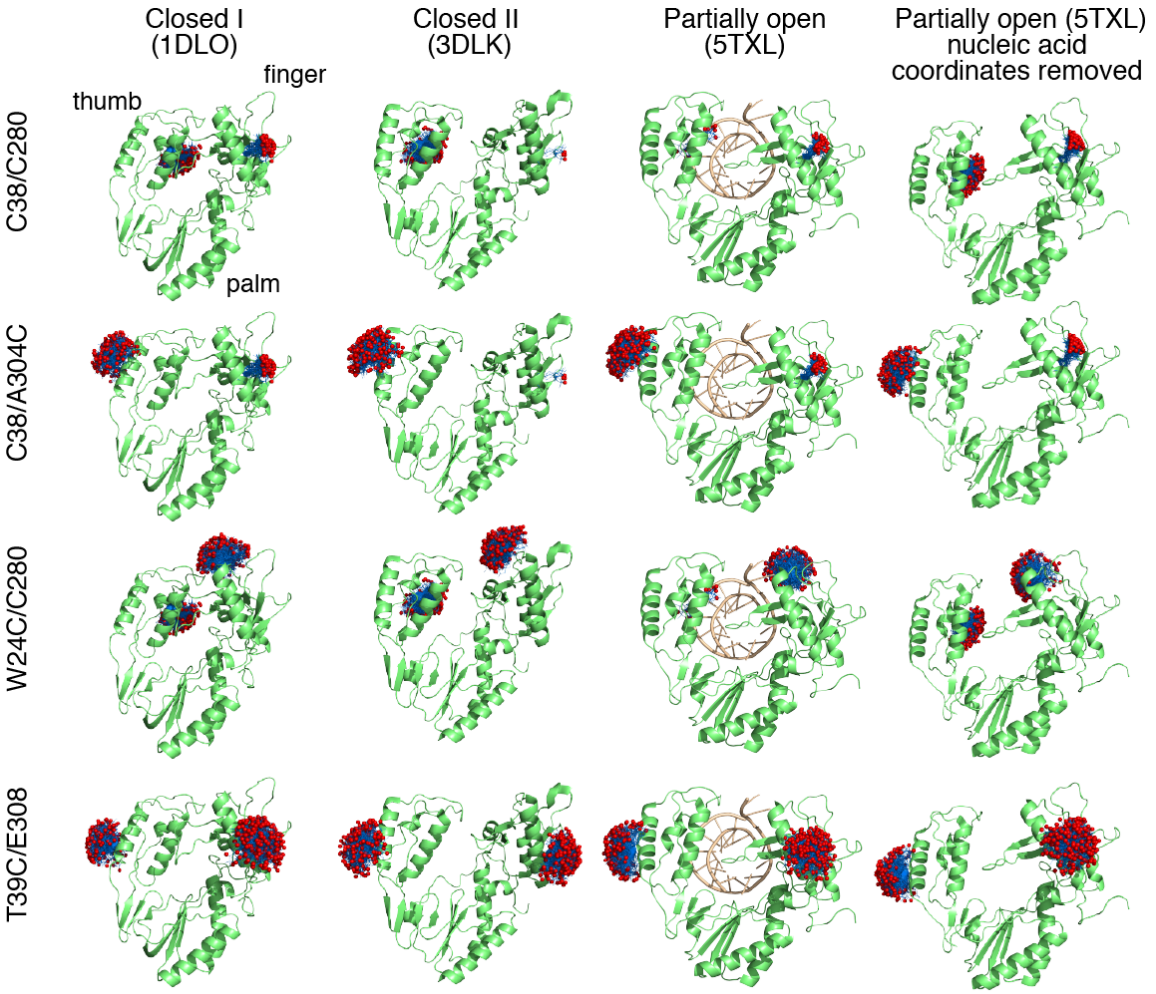

Figure S2. Distributions of nitroxide spin label sidechain rotamers in the closed I, closed II and partially-closed (with and without nucleic acid included) conformations of the finger and thumb subdomains of p66 calculated from HIV-1 RT crystal structures using the program MMM2013.2.[6]

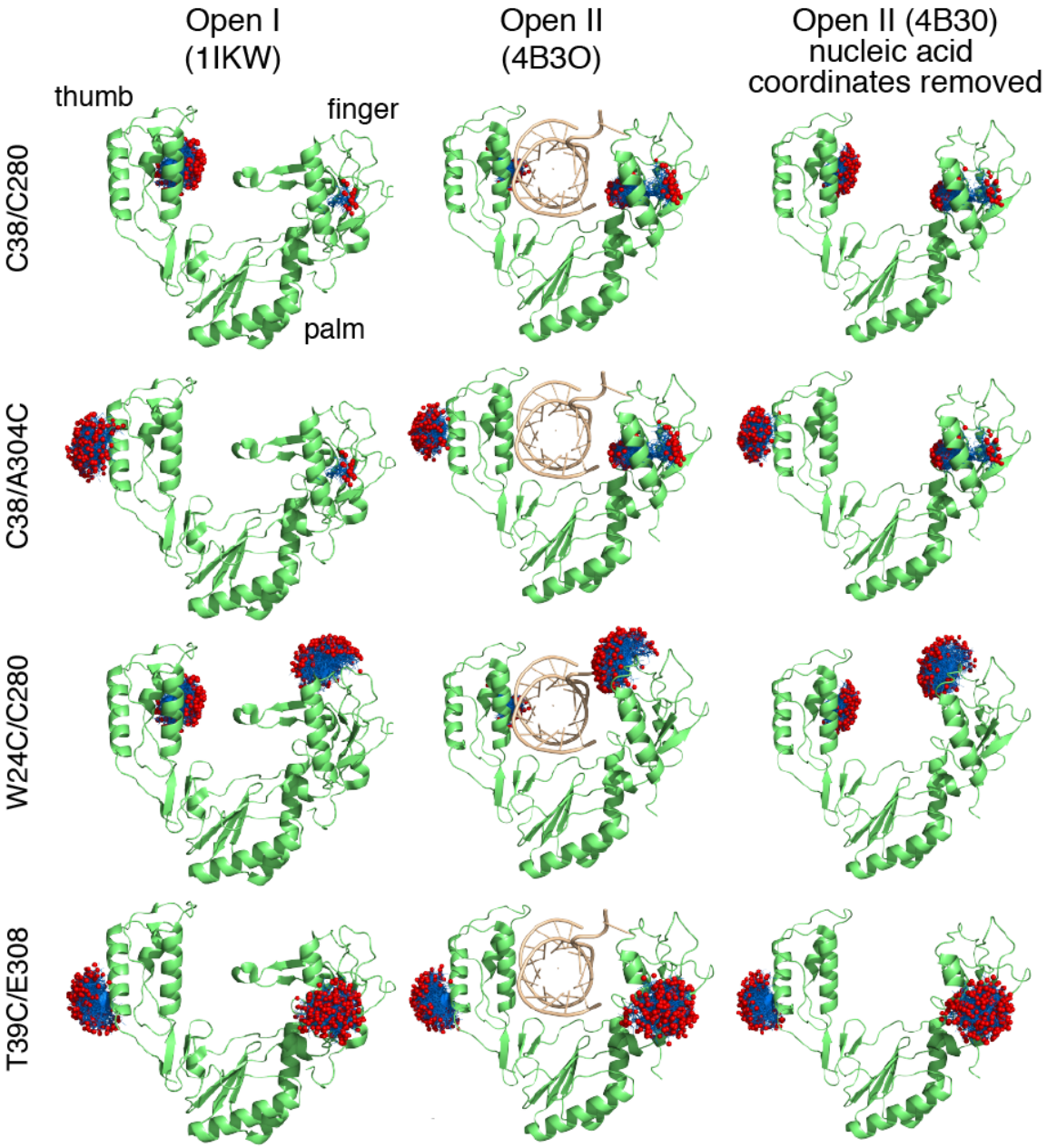

Figure S3. Distributions of nitroxide spin label sidechain rotamers in the open I and open II (with and without nucleic acid included) conformations of the finger and thumb subdomains of p66 calculated from HIV-1 RT crystal structures using the program MMM2013.2.[6]

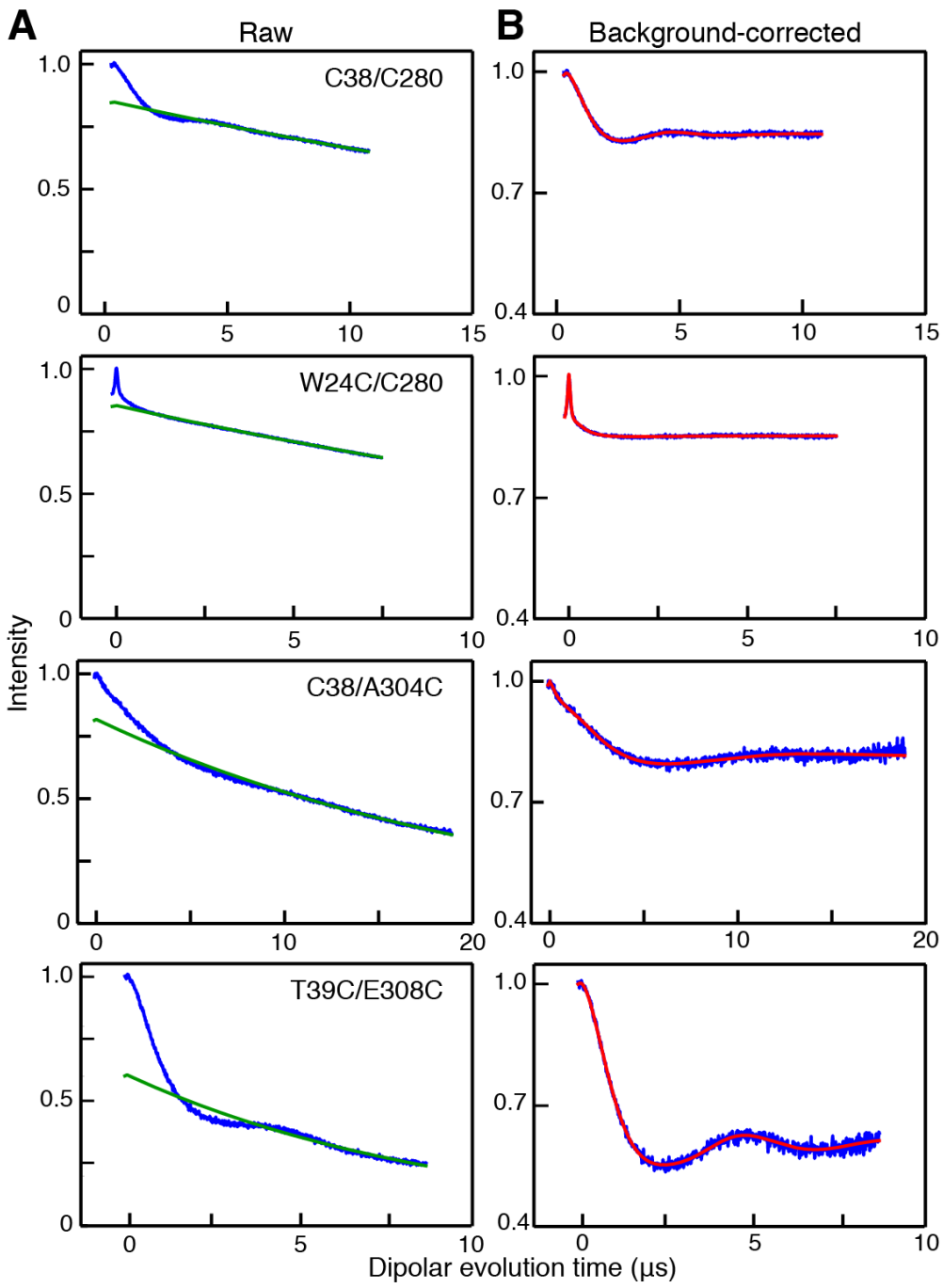

Figure S4. (A) Raw and (B) background-corrected DEER echo curves for unliganded HIV-1 RT. The experimental data are shown in blue. The DEER echo curves were fit using the DD[7] (a GUI of GLADD, Global Analysis of DEER Data) homogeneous model with an exponential background function (shown in green in panel A). Note that the theoretical normalized modulation depth (1.0 minus the value of the intercept at time = 0 for the green background function in the left panels) is 0.45 for a two-spin system with 100% spin-labeling;[1] smaller values reflect incomplete spin-labeling which, in the context of a two spin-spin system, has no impact on the DEER-derived $P(r)$ distance distributions. The best fit curves to a two Gaussian model are shown as red lines in panel (B).

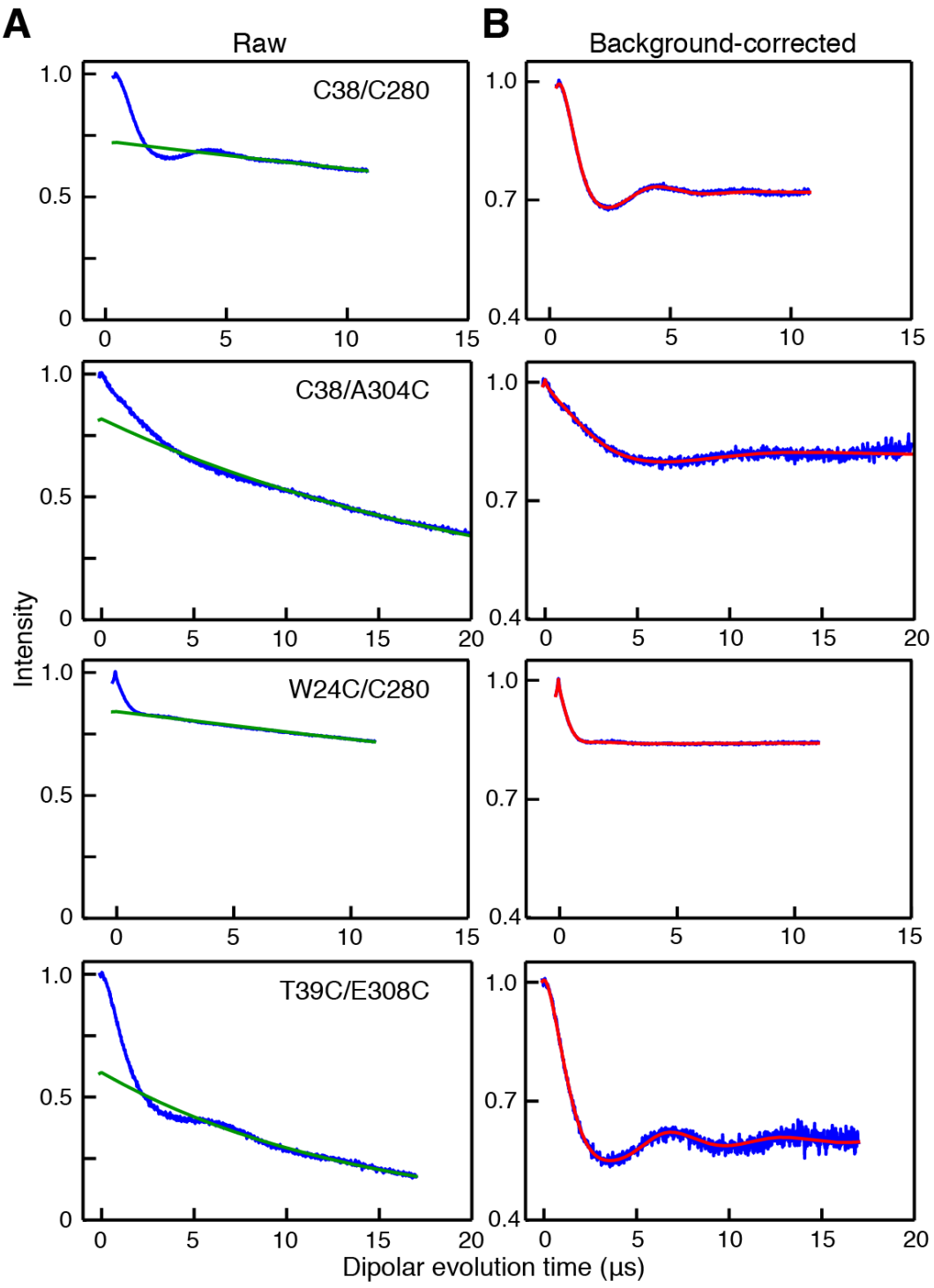

Figure S5. (A) Raw and (B) background-corrected DEER echo curves for HIV-1 RT in the presence of DNA. The experimental data are shown in blue. The DEER echo curves were fit using the DD[7] homogeneous model with an exponential background function (shown in green in panel A). The best fit curves to a two Gaussian model are shown as red lines in panel (B).

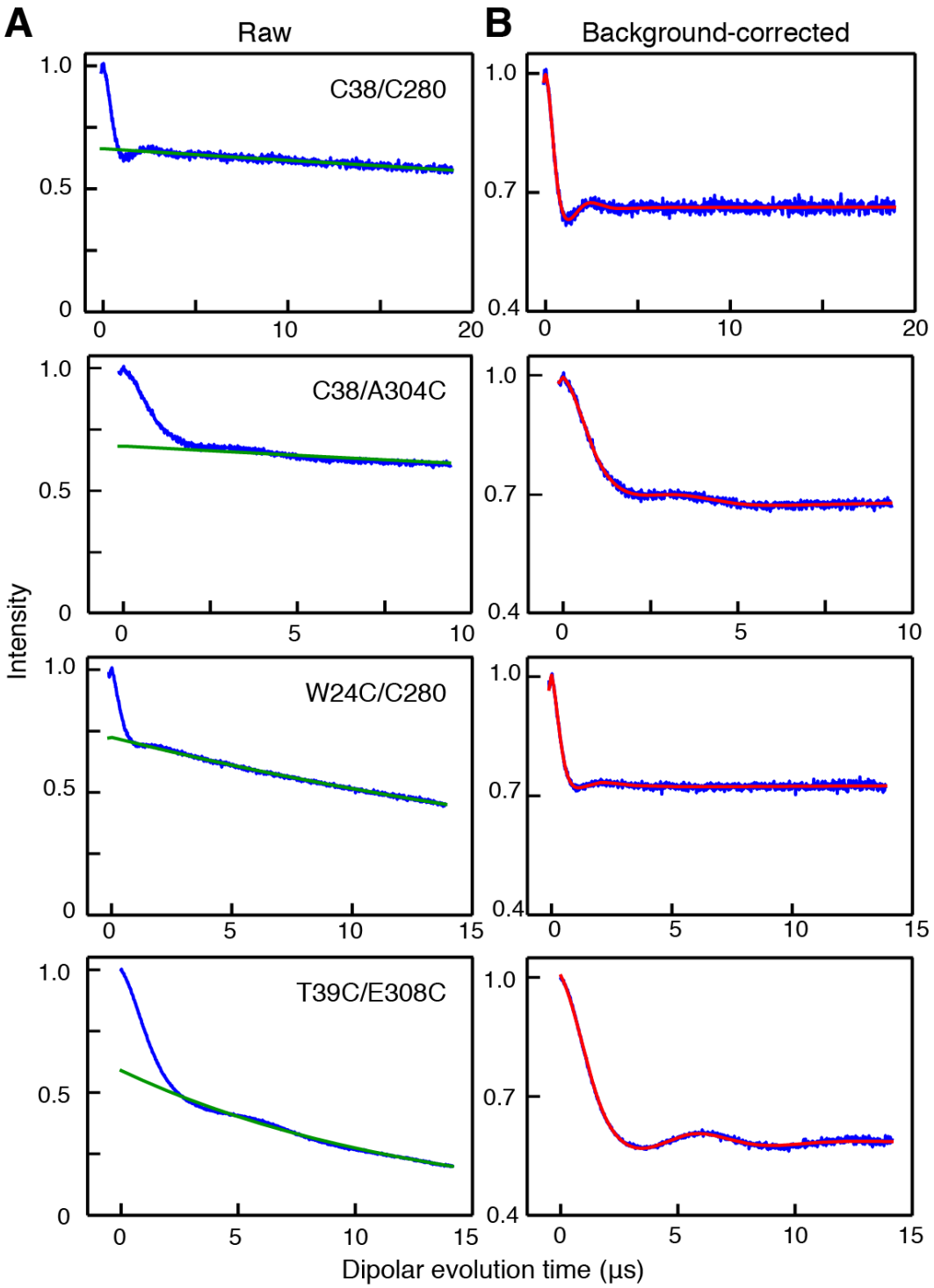

Figure S6. (A) Raw and (B) background-corrected DEER echo curves for HIV-1 RT in the presence of nevirapine. The experimental data are shown in blue. The DEER echo curves were fit using the DD[7] homogeneous model with an exponential background function (shown in green in panel A). The best fit curves to a two Gaussian model are shown as red lines in panel (B).

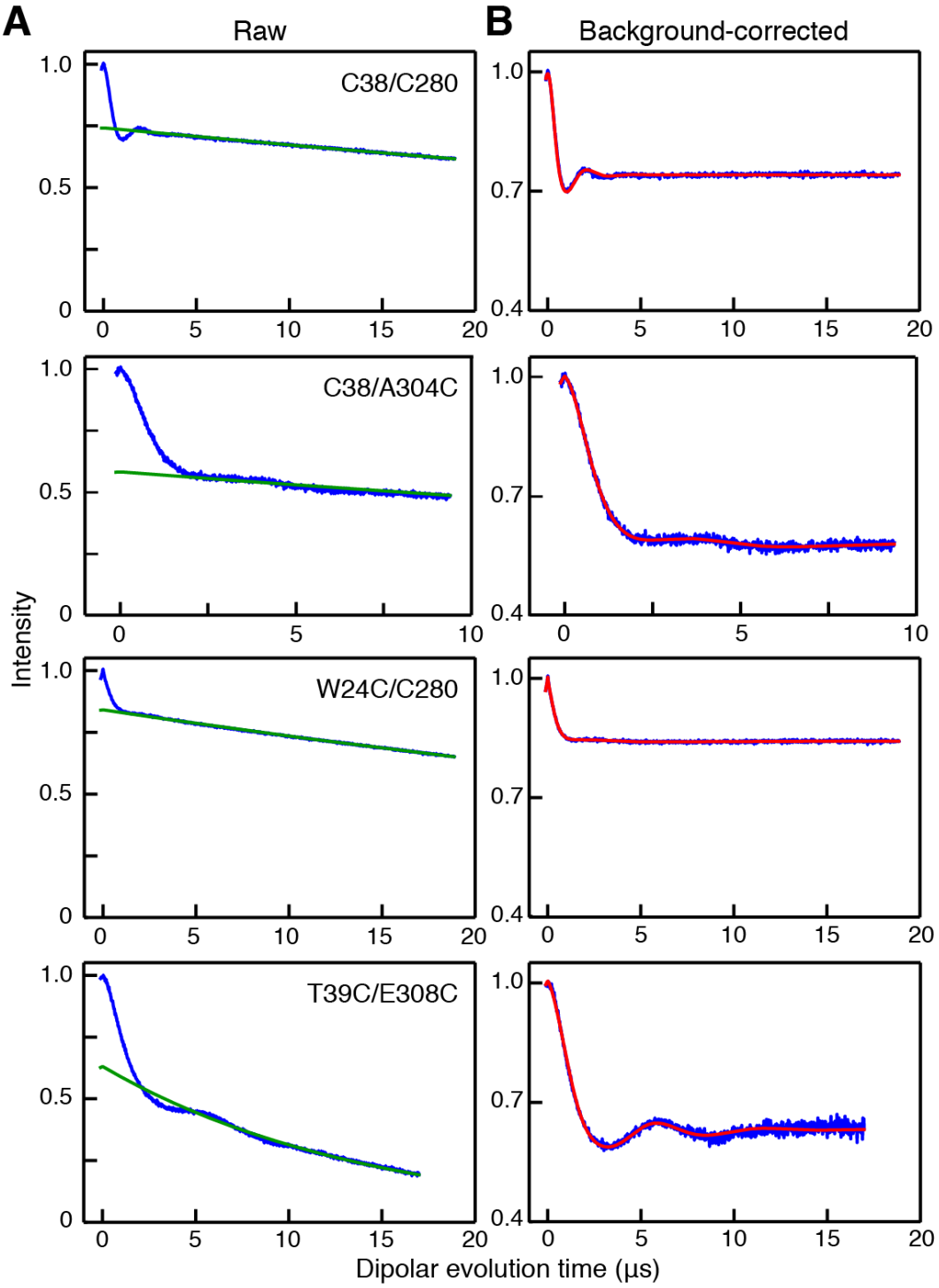

Figure S7. (A) Raw and (B) background-corrected DEER echo curves for HIV-1 RT in the presence of rilpivirine. The experimental data are shown in blue. The DEER echo curves were fit using the DD[7] homogeneous model with an exponential background function (shown in green in panel A). The best fit curves to a two Gaussian model are shown as red lines in panel (B).

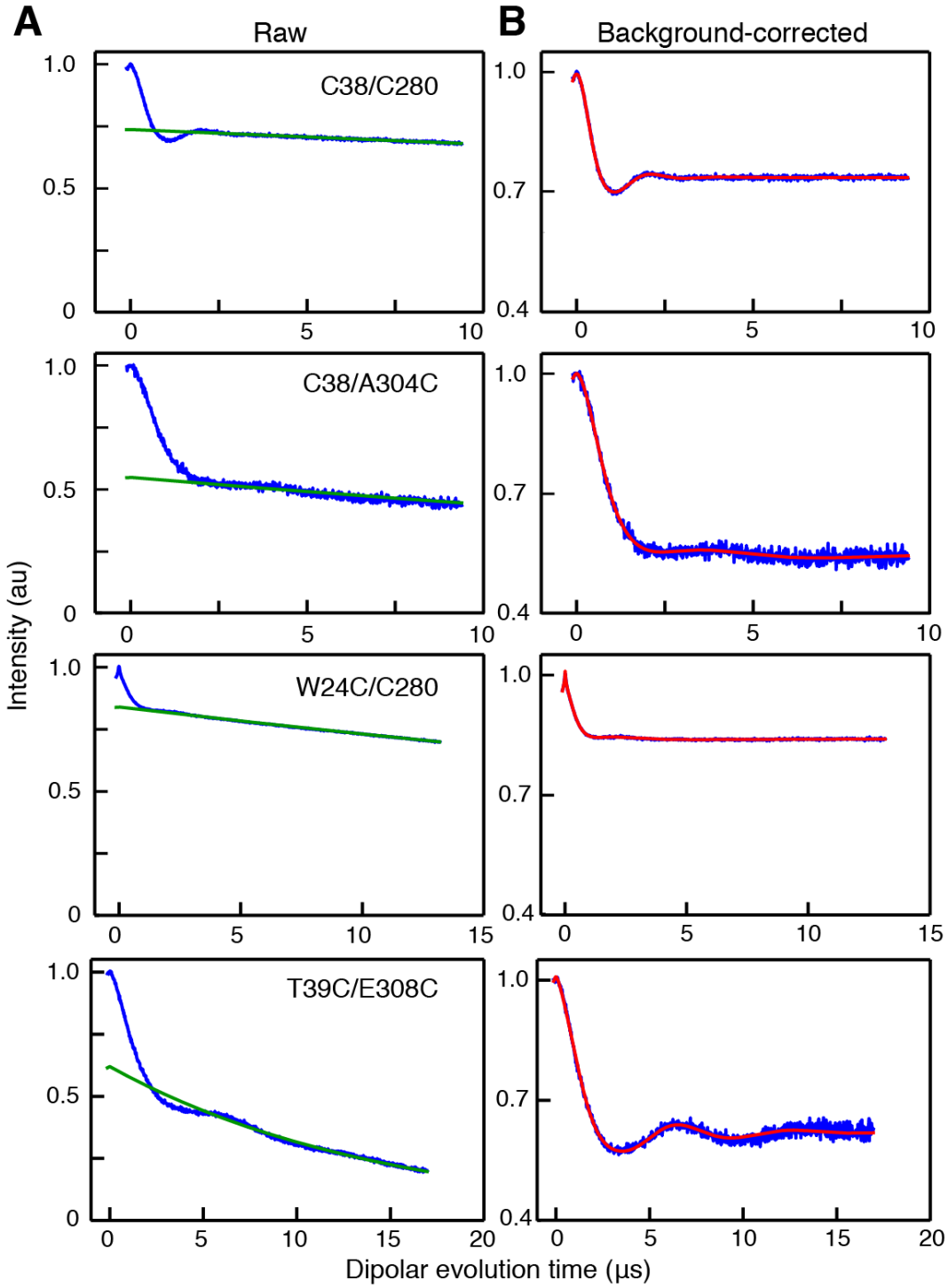

Figure S8. (A) Raw and (B) background-corrected DEER echo curves for HIV-1 RT in the presence of etravirine. The experimental data are shown in blue. The DEER echo curves were fit using the DD[7] homogeneous model with an exponential background function (shown in green in panel A). The best fit curves to a two Gaussian model are shown as red lines in panel (B).

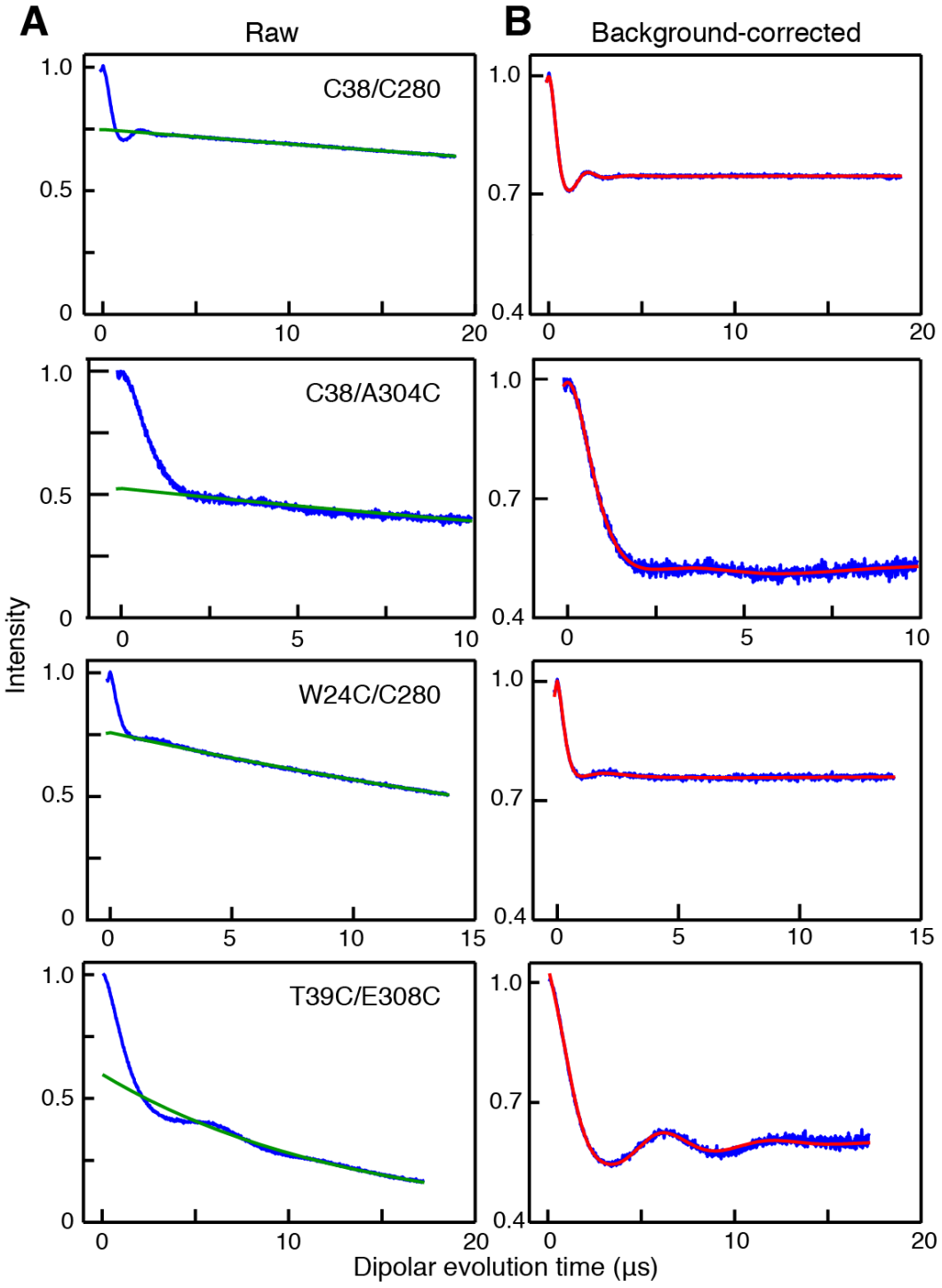

Figure S9. (A) Raw and (B) background-corrected DEER echo curves for HIV-1 RT in the presence of delavirdine. The experimental data are shown in blue. The DEER echo curves were fit using the DD[7] homogeneous model with an exponential background function (shown in green in panel A). The best fit curves to a two Gaussian model are shown as red lines in panel (B).

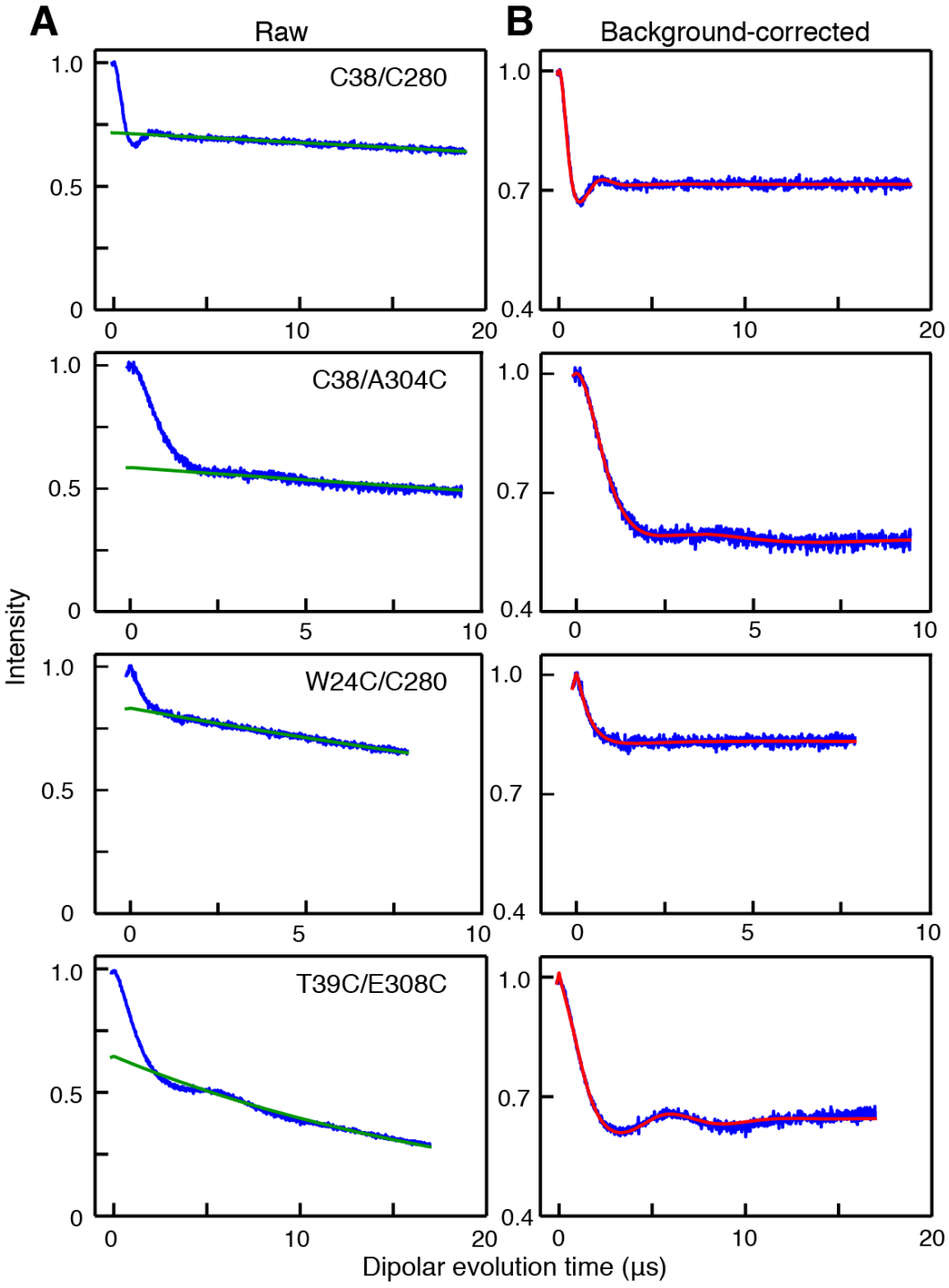

Figure S10. (A) Raw and (B) background-corrected DEER echo curves for HIV-1 RT in the presence of efavirenz. The experimental data are shown in blue. The DEER echo curves were fit using the DD[7] homogeneous model with an exponential background function (shown in green in panel A). The best fit curves to a two Gaussian model are shown as red lines in panel (B).

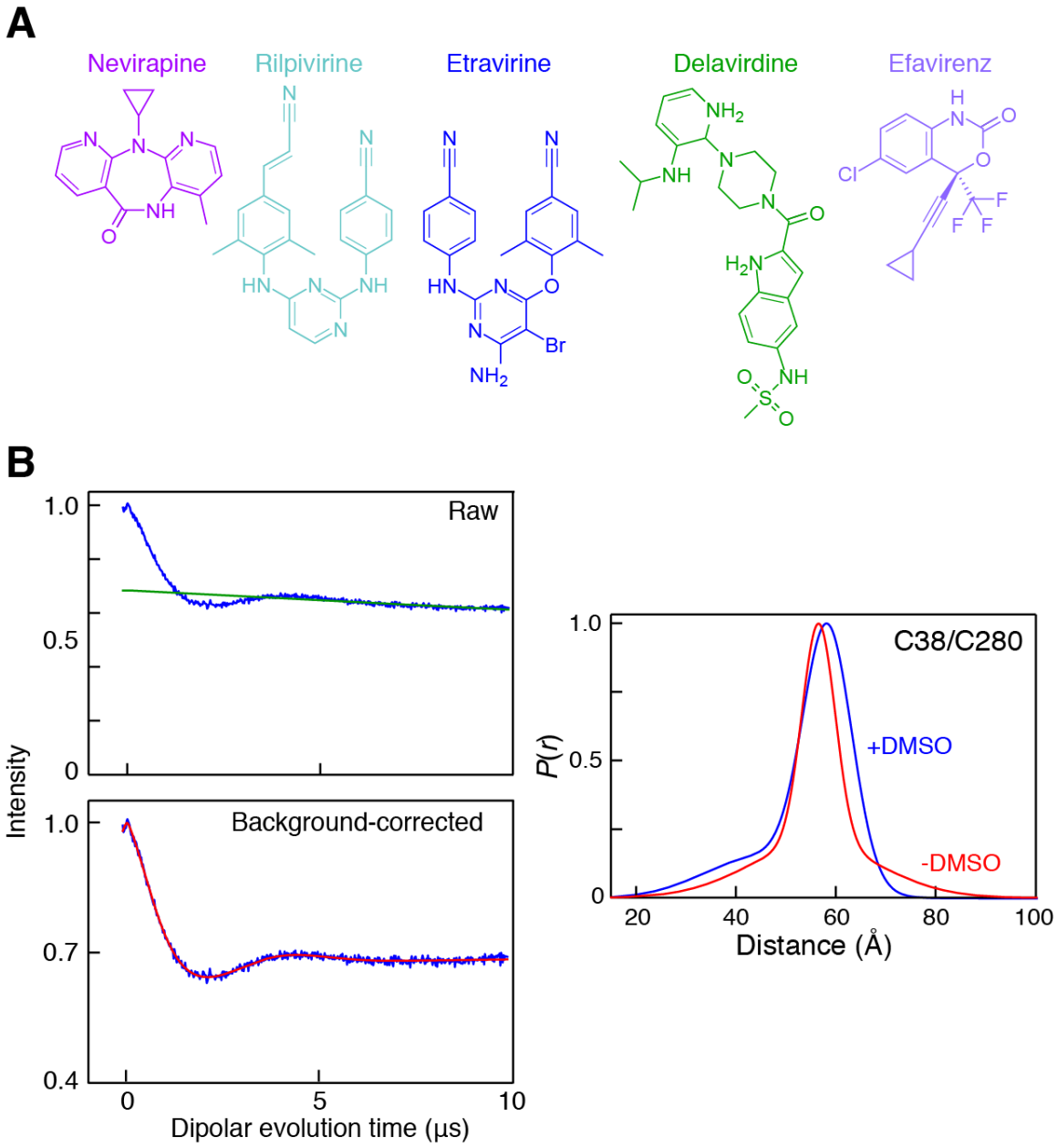

Figure S11. (A) Chemical structures of NNRTI inhibitors used in the current study. (B) Effect of DMSO on the *P*(*r*) distance distribution for C38-R1/C280-R1 unliganded HIV-1 RT. Left panels show experimental raw and background-corrected DEER echo curves for unliganded HIV-RT in the presence of 255 mM DMSO in blue. The background (green line, top panel) and best-fit curves for a two Gaussian model (red line, lower panel) obtained using DD.[7] The right panel compares the DEER-derived *P*(*r*) distance distribution between the C38-R1 and C280-R1 spin labels for unliganded HIV-RT obtained in the absence (red) and presence (blue) of DMSO. This control experiment was performed as sock solutions of NNRTIs could only be made up in DMSO

owing to poor solubility in water. The presence of DMSO has no significant impact on the $P(r)$ distance distribution.

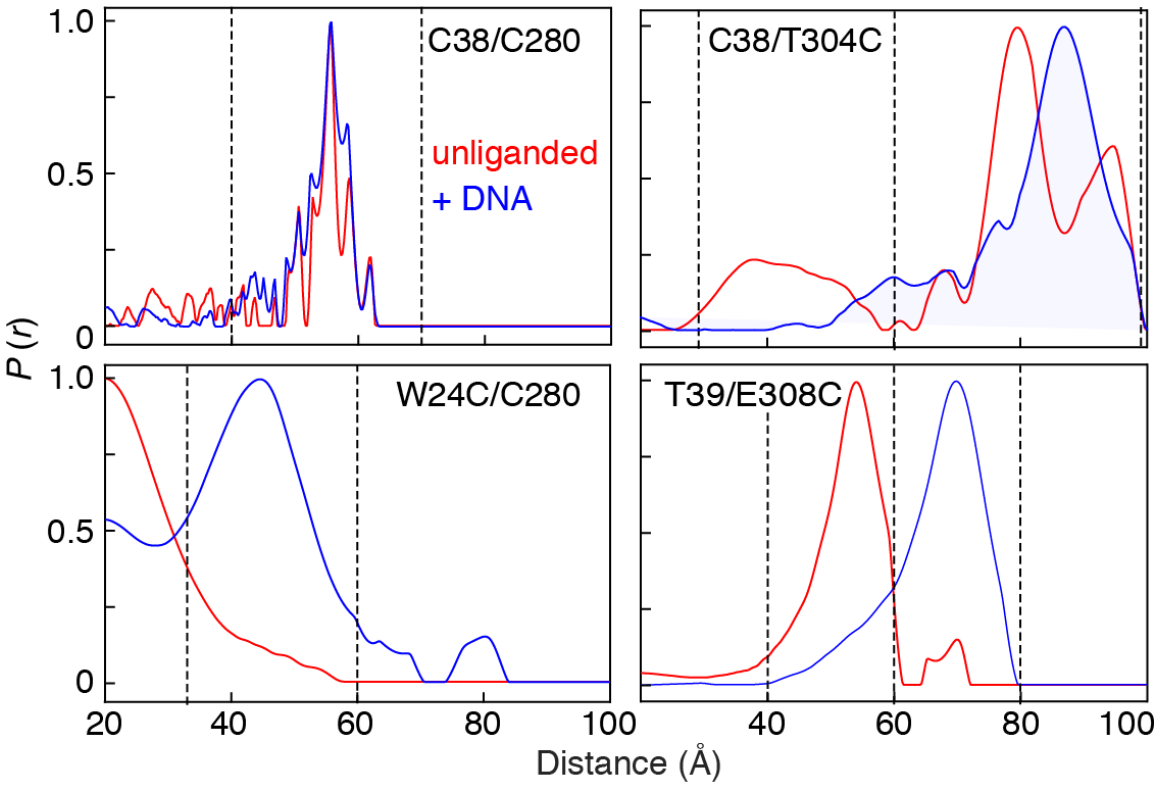

Figure S12. DEER-derived $P(r)$ distributions obtained by validated Tikhonov regularization for p66 spin-labeled HIV-RT in the absence (blue) and presence (red) of double-stranded DNA. The calculations were performed using DeerAnalysis 2016.[10] The mean distances and widths of the distance distributions reported in Table S2 are obtained for the distance intervals delineated by the dashed lines.

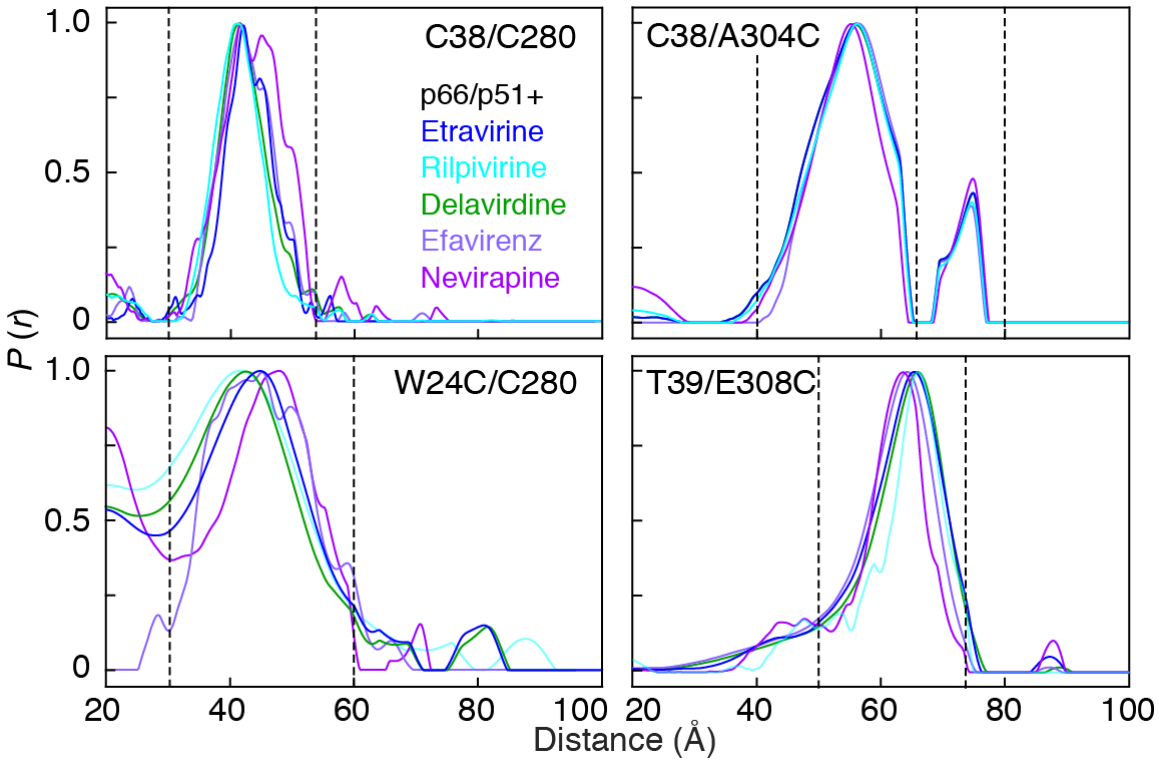

Figure S13. DEER-derived $P(r)$ distributions obtained by validated Tikhonov regularization for p66 spin-labeled HIV-RT in the presence of five different NNRTIs. The calculations were performed using DeerAnalysis 2016.[10] The mean distances and widths of the distance distributions reported in Table S2 are obtained for the distance intervals delineated by the dashed lines.

Supplementary References

[1] Schmidt, T., Ghirlando, R., Baber, J., and Clore, G. M. (2016) *ChemPhysChem 17*, 2987-2991.

[2] Schneider, A., Corona, A., Sporing, I., Jordan, M., Buchholz, B., Maccioni, E., Di Santo, R., Bodem, J., Tramontano, E., and Wohrl, B. M. (2016) *Nucleic Acids Res. 44*, 2310-2322.

[3] Bohlayer, W. P., and DeStefano, J. J. (2006) *Biochemistry 45*, 7628-7638.

[4] Pannier, M., Veit, S., Godt, A., Jeschke, G., and Spiess, H. W. (2000) *J. Magn. Reson. 142*, 331-340.

[5] Baber, J. L., Louis, J. M., and Clore, G. M. (2015) *Angew. Chem. Int. Ed. Engl. 54*, 5336-5339.

[6] Polyhach, Y., Bordignon, E., and Jeschke, G. (2011) *Phys. Chem. Chem. Phys. 13*, 2356-2366.

[7] Brandon, S., Beth, A. H., and Hustedt, E. J. (2012) The global analysis of DEER data, *J. Magn. Reson. 218*, 93-104.

[8] Stein, R. A., Beth, A. H., and Hustedt, E. J. (2015) *Methods Enzymol. 563*, 531-567.

[9] Claxton, D. P., Kazmier, K., Mishra, S., and Mchaourab, H. S. (2015) *Methods Enzymol. 564*, 349-387.

[10] Jeschke, G., Chechik, V., Ionita, P., Godt, A., Zimmermann, H., Banham, J., Timmel, C. R., Hilger, D., and Jung, H. (2006) *App. Magn. Reson. 30*, 473-498.

[11] Fischer, M., Lifshitz, R., Katz, T., Liefer, I., Ben-Artzi, H., Gorecki, M., Panet, A., and Zeelon, E. (1992) *Protein Expr. Purif. 3*, 301-307.

[12] Hsiou, Y., Ding, J., Das, K., Clark, A. D., Jr., Hughes, S. H., and Arnold, E. (1996) *Structure 4*, 853-860.

[13] Hsiou, Y., Ding, J., Das, K., Clark, A. D., Jr., Boyer, P. L., Lewi, P., Janssen, P. A., Kleim, J. P., Rosner, M., Hughes, S. H., and Arnold, E. (2001) *J. Mol. Biol. 309*, 437-445.

[14] Das, K., Sarafianos, S. G., Clark, A. D., Jr., Boyer, P. L., Hughes, S. H., and Arnold, E. (2007) *J. Mol. Biol. 365*, 77-89.

[15] Ren, J., Bird, L. E., Chamberlain, P. P., Stewart-Jones, G. B., Stuart, D. I., and Stammers, D. K. (2002) *Proc. Natl. Acad. Sci. U. S. A. 99*, 14410-14415.

[16] Nakamura, A., Tamura, N., and Yasutake, Y. (2015) *Acta Crystallogr. F Struct. Biol. Commun. 71*, 1384-1390.

[17] Sarafianos, S. G., Das, K., Clark, A. D., Jr., Ding, J., Boyer, P. L., Hughes, S. H., and Arnold, E. (1999) *Proc. Natl. Acad. Sci. U. S. A. 96*, 10027-10032.

[18] Bauman, J. D., Das, K., Ho, W. C., Baweja, M., Himmel, D. M., Clark, A. D., Jr., Oren, D. A., Boyer, P. L., Hughes, S. H., Shatkin, A. J., and Arnold, E. (2008) *Nucleic Acids Res. 36*, 5083-5092.

[19] Himmel, D. M., Maegley, K. A., Pauly, T. A., Bauman, J. D., Das, K., Dharia, C., Clark, A. D., Jr., Ryan, K., Hickey, M. J., Love, R. A., Hughes, S. H., Bergqvist, S., and Arnold, E. (2009) *Structure 17*, 1625-1635.

[20] Hachiya, A., Marchand, B., Kirby, K. A., Michailidis, E., Tu, X., Palczewski, K., Ong, Y. T., Li, Z., Griffin, D. T., Schuckmann, M. M., Tanuma, J., Oka, S., Singh, K., Kodama, E. N., and Sarafianos, S. G. (2012) *J. Biol. Chem. 287*, 29988-29999.

[21] Das, K., Martinez, S. E., and Arnold, E. (2017) *Antimicrob. Agents Chemother. 61*. e00224-17.

[22] Das, K., Martinez, S. E., Bauman, J. D., and Arnold, E. (2012) *Nature Struct. Mol. Biol. 19*, 253-259.

[23] Lansdon, E. B., Samuel, D., Lagpacan, L., Brendza, K. M., White, K. L., Hung, M., Liu, X., Boojamra, C. G., Mackman, R. L., Cihlar, T., Ray, A. S., McGrath, M. E., and Swaminathan, S. (2010) *J. Mol. Biol. 397*, 967-978.

[24] Lansdon, E. B., Liu, Q., Leavitt, S. A., Balakrishnan, M., Perry, J. K., Lancaster-Moyer, C., Kutty, N., Liu, X., Squires, N. H., Watkins, W. J., and Kirschberg, T. A. (2011) *Antimicrob. Agents Chemother. 55*, 2905-2915.

[25] Lindberg, J., Sigurdsson, S., Lowgren, S., Andersson, H. O., Sahlberg, C., Noreen, R., Fridborg, K., Zhang, H., and Unge, T. (2002) *Eur. J. Biochem. 269*, 1670-1677.

[26] Kuroda, D. G., Bauman, J. D., Challa, J. R., Patel, D., Troxler, T., Das, K., Arnold, E., and Hochstrasser, R. M. (2013) *Nature Chem. 5*, 174-181.

[27] Esnouf, R. M., Ren, J., Hopkins, A. L., Ross, C. K., Jones, E. Y., Stammers, D. K., and Stuart, D. I. (1997) *Proc. Natl. Acad. Sci. U. S. A. 94*, 3984-3989.

[28] Das, K., Clark, A. D., Jr., Lewi, P. J., Heeres, J., De Jonge, M. R., Koymans, L. M., Vinkers, H. M., Daeyaert, F., Ludovici, D. W., Kukla, M. J., De Corte, B., Kavash, R. W., Ho, C. Y., Ye, H., Lichtenstein, M. A., Andries, K., Pauwels, R., De Bethune, M. P., Boyer, P. L., Clark, P., Hughes, S. H., Janssen, P. A., and Arnold, E. (2004) *J. Med. Chem. 47*, 2550-2560.

[29] Ren, J., Nichols, C., Bird, L., Chamberlain, P., Weaver, K., Short, S., Stuart, D. I., and Stammers, D. K. (2001) *J. Mol. Biol. 312*, 795-805.

[30] Lapkouski, M., Tian, L., Miller, J. T., Le Grice, S. F. J., and Yang, W. (2013) *Nat. Struct. Mol. Biol. 20*, 230-236.

[31] Das, K., Martinez, S. E., Bauman, J. D., and Arnold, E. (2012) *Nat. Struct. Mol. Biol. 19*, 253-259.